Magnetovolume effect and magnetic properties of $Dy_2Fe_{17-x}Mn_x$

J. L. Wang,[1,3] S. J. Campbell,[1] O. Tegus,[2] C. Marquina,[3] and M. R. Ibarra[3]
[1]*School of Physical, Environmental and Mathematical Sciences, The University of New South Wales, The Australian Defence Force Academy, Canberra ACT 2600, Australia*
[2]*Van der Waals-Zeeman Institute, University of Amsterdam, 1018 XE Amsterdam, The Netherlands*
[3]*Departmento de Física de la Materia Condensada-Instituto de Ciencia de Materiales de Aragón, Universidad de Zaragoza-CSIC, Pedro Cerbuna 12, 50009 Zaragoza, Spain*
(Received 1 October 2006; revised manuscript received 16 February 2007; published 17 May 2007)

The structural and magnetic properties of $Dy_2Fe_{17-x}Mn_x$ (x=0–5) compounds have been investigated using x-ray diffraction, linear thermal expansion, magnetization measurements, and ^{57}Fe Mössbauer spectroscopy. Compared with $Dy_2Co_{17-x}Mn_x$ compounds for which a linear increase of the unit-cell volume V with increasing Mn fraction is found, the compositional dependence of the lattice parameters of $Dy_2Fe_{17-x}Mn_x$ first exhibits a slight maximum around x=0.5 before increasing monotonically with further increase in x; this behavior can be ascribed to a spontaneous magnetostriction as confirmed by linear-thermal-expansion measurements. The Curie temperature T_C remains essentially unchanged for Mn contents up to x=1 [T_C=370(4) K for x=0.0, T_C=373(4) K for x=1.0] before decreasing steadily with further increase in Mn content [T_C=232(4) K for $Dy_2Fe_{12}Mn_5$]. The rapid decrease of spontaneous magnetization and the essentially constant value of T_C for lower Mn concentrations can be understood in terms of the two-sublattice model and by considering the preferential site occupation of Mn atoms in the $Dy_2Fe_{17-x}Mn_x$ unit cell. The exchange interaction between the rare-earth and transition-metal sublattices has been investigated by means of a mean-field analysis of the high-field magnetization isotherms which were measured on the powder samples. The ^{57}Fe hyperfine interaction parameters of the $Dy_2Fe_{16}Mn_1$ and $Dy_2Fe_{14}Mn_3$ samples have been determined from the Mössbauer spectra (5–300 K).

DOI: 10.1103/PhysRevB.75.174423 PACS number(s): 75.30.Gw, 75.50.Gg, 75.30.Et, 75.30.Cr

I. INTRODUCTION

Intermetallic compounds based on rare-earth (R) and 3*d* transition-metal elements (T) form a large family of materials that are important both from the technological and fundamental points of view.[1] In the past few decades, many investigations have been carried out on R_2T_{17} compounds with the main aims being to understand and improve their magnetic properties with possible practical applications as high-energy-product magnets in mind.[1] R_2T_{17} compounds (T=Fe or Co) crystallize either in the rhombohedral structure (*R*-3*m* space group, Th_2Zn_{17}-like with a single R site 6*c* and four different T sites 6*c*, 9*d*, 18*f*, and 18*h*) for light rare earths or in the hexagonal structure for heavy rare earths [*P*6(3)/*mmc* space group, Th_2Ni_{17}-like with two R sites 2*b* and 2*d* and four T sites 4*f*, 6*g*, 12*j*, and 12*k*]. The change of structure usually occurs at R=Gd and results from the lanthanide contraction.[1] Both hexagonal and rhombohedral structures can be derived from the $CaCu_5$-type structure by the ordered substitution of one-third of rare-earth atoms by a pair (dumbbell) of T atoms.[1]

The magnetic properties of R_2Fe_{17}- and R_2Co_{17}-based solid solutions can be modified by partially substituting Fe or Co with other magnetic or nonmagnetic elements, such as Al,[2–4] Ga,[5–8] Si,[6,9,10] or Mn.[4,11–18] Due to the existence of competing ferromagnetic and antiferromagnetic interactions within the same sublattice of the 3*d* metal atoms in the R_2Fe_{17}-based compounds, the substitution of a third element for Fe in R_2Fe_{17} has a significant influence on the Curie temperature T_C and other related magnetic properties.[3,5,6,8,17] On the other hand, due to the presence of such "dumbbell" sites (6*c* in Th_2Zn_{17}-type structure or 4*f* in Th_2Ni_{17}-type structure) in the corresponding R_2Co_{17} compounds,[2] the different influence on structural and magnetic properties resulting from the introduction of T atoms should be expected in $R_2Co_{17-x}T_x$ compounds.[2,15,18] In fact, it was found that the compositional dependence of lattice parameters in $R_2Fe_{17-x}Mn_x$ compounds[11,13,14,17] exhibits a behavior different from that found in $R_2Co_{17-x}Mn_x$ (Refs. 15 and 18) for a small amount of Mn substitution. Because Mn atoms preferentially occupy the dumbbell pair sites which have the largest Wigner-Seitz cell (WSC) volume, some authors ascribed the unexpected composition dependence of lattice volume with Mn content in $R_2Fe_{17-x}Mn_x$ compounds to this preferential occupation of Mn atoms,[12,15] while other authors thought that the magnetovolume effect should be responsible for this anomaly.[4,13,17] Here, we investigate the effects of replacing Fe by Mn on the volume and magnetic properties of $Dy_2Fe_{17-x}Mn_x$ (lattice parameters, magnetization, and exchange interactions) and show that magnetovolume effects are the major reason for this anomalous composition dependence of the lattice parameters with Mn content.

II. EXPERIMENT

$Dy_2Fe_{17-x}Mn_x$ alloys with x=0, 0.5, 1.0, 2.0, 3.0, 4.0, and 5.0 were prepared by arc-melting of 99.9% purity materials in argon atmosphere. The ingots were annealed in argon atmosphere at 1273 K for 24 h, followed by quenching in water. A small amount (less than 3%) of Mn was added to compensate for the loss of Mn during arc-melting and the subsequent annealing processes. X-ray diffraction with

TABLE I. Magnetic parameters of $Dy_2Fe_{17-x}Mn_x$ compounds ($x=0-5.0$) as discussed in the text: T_C from M^2-T plots or thermal-expansion measurements; critical temperature T_{cr} and freezing temperature T_f; spontaneous magnetization M_s and transition-metal sublattice magnetization M_T at 5 K; intersublattice molecular coefficient n_{RT}. (Uncertainties for T_C, T_{cr}, and T_f values are ±4 K and for M_s and M_T values ±0.1 μ_B/f.u.)

Mn content x	T_C (K) (M^2-T)	T_C (K) (thermal expansion)	T_{cr} (K)	T_f (K)	M_s (5 K) (μ_B/f.u.)	M_T (5 K) (μ_B/f.u.)	n_{RT} (T f.u./μ_B)
0.0		370			16.6	36.6	
0.5		375			14.6	34.6	
1.0		373	16	319	12.1	32.1	
2.0	349	351	48	311	6.5	26.5	
3.0	310	309	73	261	2.1	22.1	3.61
4.0	256		104		0.9	19.1	3.91
5.0	232		35		5.3	14.7	3.96

Cu $K\alpha$ radiation was employed to check if the samples were single phase and to determine the lattice parameters. Thermal-expansion measurements were performed using a "push-rod" linear differential transformer method in the temperature range 100–650 K.[17] The temperature dependences of the magnetization $M(T)$ were measured in an applied magnetic field of 0.05 T in a superconducting quantum interference device from 5 to 350 K on fixed powder samples. The Curie temperatures T_C for $Dy_2Fe_{17-x}Mn_x$ samples with $x=2.0$, 3.0, 4.0, 5.0 (T_C below 350 K) were derived from M^2-T plots by extrapolating M^2 to zero, while the T_C values for samples with $x=0$, 0.5, 1.0 (T_C above 350 K) were determined from the minimum of the coefficient of linear thermal expansion (data summarized in Table I).

Magnetization measurements in fields up to 38 T at 4.2 K were performed in the High Magnetic Field Installation at the University of Amsterdam.[6,8] The high-field measurements were done on powder samples consisting of particles of about 30 μm size, which are sufficiently small to regard them as monocrystalline.[19] During the high-field magnetization measurements, the particles are free to rotate in the sample holder, so that they can orient their magnetic moments parallel to the applied field.[6,19–21] This procedure enables us to accurately evaluate the R-T exchange interaction in the ferrimagnetic R-T compounds as the ferrimagnetic structure may be destroyed and a steep increase in the magnetization appears if the external field is high enough.[19] The exchange interaction constants can then be determined in a straightforward manner as discussed in Sec. III B. ^{57}Fe Mössbauer spectra were obtained for the $Dy_2Fe_{16}Mn$ and $Dy_2Fe_{14}Mn_3$ compounds between 4.5 and 298 K using a standard constant-acceleration spectrometer and a ^{57}CoRh source. The spectrometer was calibrated at room temperature with an α-iron foil.

III. RESULTS AND DISCUSSION

A. Structural properties

Thermomagnetic and x-ray powder diffraction analyses indicate that all of the $Dy_2Fe_{17-x}Mn_x$ samples investigated are single phase. As shown in Fig. 1(a), the x-ray powder diffraction patterns reveal that samples with $x<3.0$ crystallize in the Th_2Ni_{17}-type structure, while for samples with $x \geqslant 3.0$ a coexistence of the Th_2Ni_{17} and Th_2Zn_{17} structures occurs [representative x-ray-diffraction patterns are shown for $x=0.0$, 0.5, 1.0, and 3.0 in Fig. 1(a)]. A similar situation occurs in $R_2Fe_{17-x}M_x$ with M=Al, Ga, and Si where the Th_2Ni_{17} structure becomes unstable with increasing M content.[3,8–10]

The lattice parameters a and c (determined using the standard pattern matching method of the FULLPROF program[22]) and the unit-cell volume V for the $Dy_2Fe_{17-x}Mn_x$ samples at room temperature are shown in Fig. 1(b). In order to compare the c values of the hexagonal structures with those corresponding to the rhombohedral structures [a^* and c^* in Fig. 1(b) represent the lattice parameters for the rhombohedral structure], the latter are multiplied by 2/3. In comparison with $R_2Fe_{17-x}M_x$ (M=Al,Ga,Si) (Refs. 3 and 8–10)—for which the unit-cell volumes change monotonically with M content [increase for Al or Ga,[3,8] decrease for Si (radius =1.17 Å)[9,10]—Fig. 1(b) reveals that the replacement of Mn for Fe in $Dy_2Fe_{17-x}Mn_x$ leads initially to a slight maximum around $x=0.5$ before giving way to a monotonic increase in the unit-cell volume for $x \geqslant 2$. Given that Mn atoms (radius =1.35 Å)—such as Al (1.43 Å) and Ga (1.41 Å)—are larger than Fe atoms (1.26 Å), this behavior in the composition dependence of the lattice parameters is unexpected. It has been reported that Al or Ga atoms preferentially occupy the $18h/12k$ and $18f/12j$ sites at low Al concentration,[3,7] while the $6c/4f$ sites that have the largest Wigner-Seitz cell volumes are preferentially occupied by Mn atoms for small amounts of Mn substitution.[7,11,12] The nonmonotonic compositional dependence of the unit-cell volume in $R_2Fe_{17-x}Mn_x$ has been ascribed to different Mn site occupancy factors depending on the Mn content. However, it has also been reported that Mn atoms have a similar preferential occupancy for $6c/4f$ sites in $R_2Co_{17-x}Mn_x$ (Refs. 23 and 24) and $R_2Fe_{17-x}Mn_x$ (Refs. 11, 12, and 16). Therefore, the compositional dependences of the lattice parameters as shown in Fig. 1(b) for $Dy_2Fe_{17-x}Mn_x$ imply that besides the influence of preferential site occupancies of Mn atoms, other factors may

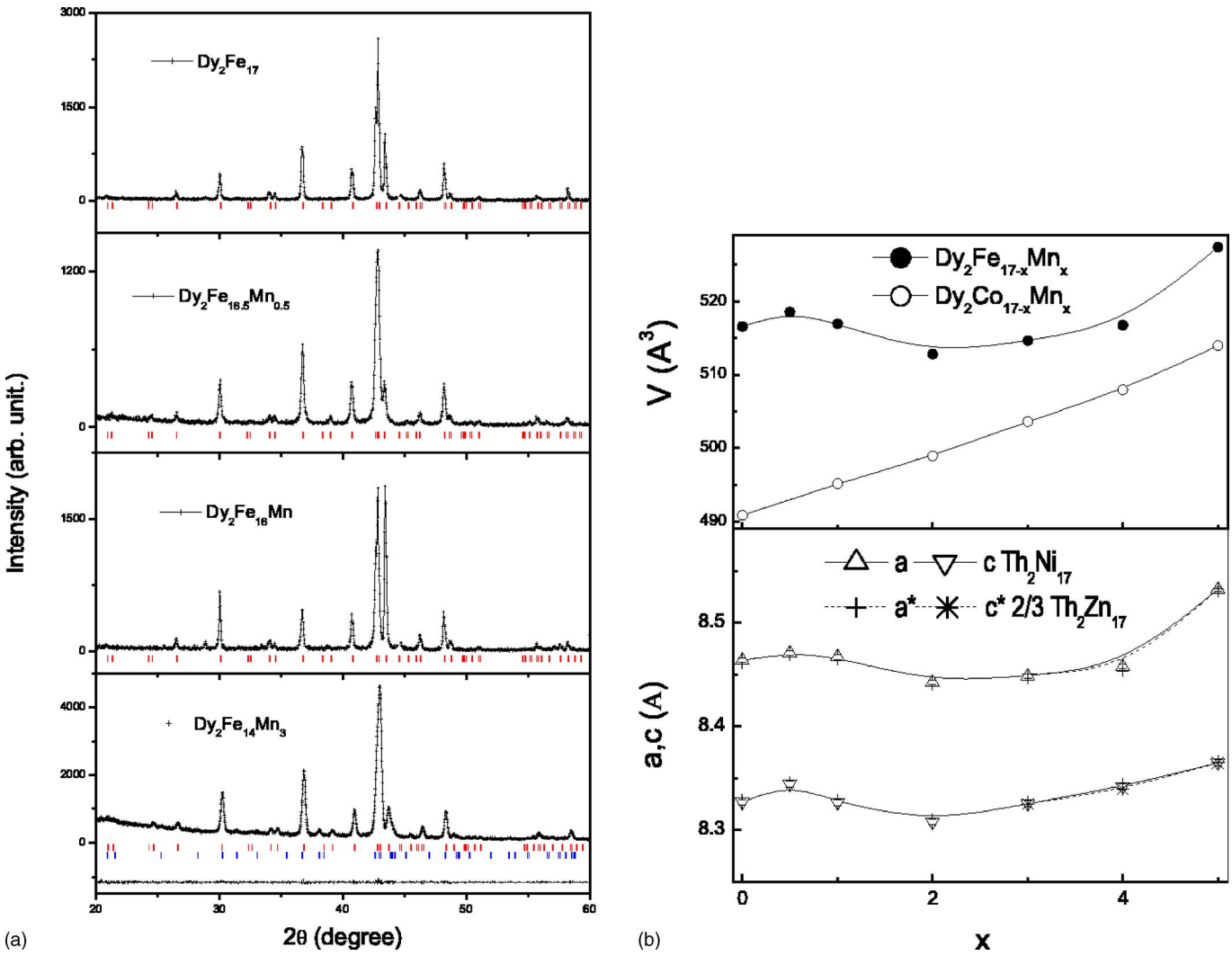

FIG. 1. (Color online) (a) X-ray-diffraction patterns (Cu $K\alpha$ radiation) for $Dy_2Fe_{17-x}Mn_x$ compounds ($x=0,0.5,1,3$). As discussed in the text, Dy_2Fe_{17}, $Dy_2Fe_{16.5}Mn_{0.5}$, and $Dy_2Fe_{16}Mn_1$ exhibit the Th_2Ni_{17}-type structure of Bragg peak positions indicated by the markers, while $Dy_2Fe_{14}Mn_3$ exhibits coexistence of the Th_2Ni_{17}-type and Th_2Zn_{17}-type structures (upper markers for Th_2Ni_{17} type, lower markers for the Th_2Zn_{17} type). (b) Compositional dependence of the lattice parameters a and c and the unit-cell volume V at room temperature of $Dy_2Fe_{17-x}Mn_x$ compounds (a^* and c^* represent the lattice parameters for the rhombohedral structure). The behavior of the unit-cell volume of $Dy_2Co_{17-x}Mn_x$ is shown for comparison (Ref. 18).

contribute to the nonmonotonic dependence of the cell volume on the Mn content in $Dy_2Fe_{17-x}Mn_x$ [the monotonic behavior of the unit-cell volume of $Dy_2Co_{17-x}Mn_x$ (Ref. 18) is shown for comparison in Fig. 1(b)].

In order to clarify this nonmonotonic behavior, we have measured the linear thermal expansion (LTE) on the $Dy_2Fe_{17-x}Mn_x$ compounds with T_C close to or above room temperature using the push-rod method.[17,25] The measurements were performed up to very high temperature (far above T_C) in order to obtain the nonmagnetic contribution. In Fig. 2(a), we show the temperature dependence of the $\Delta l/l(T)$ and the LTE coefficient, $\alpha(T)=l^{-1}(\Delta l/\Delta T)$.[25] It can be seen that the $\Delta l/l(T)$ tends toward a linear behavior at high temperatures and both the $\Delta l/l(T)$ and $\alpha(T)$ exhibit a clear invarlike anomaly around the Curie temperature.[17] The magnetic contribution to the thermal expansion, $[\Delta l/l(T)]_m$, which gives rise to the invar behavior can be obtained by comparing the experimental results with the lattice thermal contribution, $[\Delta l/l(T)]_{latt}$. This contribution can be calculated through the Grüneisen relation: $\alpha_{nm}(T)=\kappa\gamma C_v(T)/3$, where α_{nm} is the phonon anharmonic LTE coefficient, κ the isothermal compressibility, γ the Grüneisen parameter, and C_v the specific heat. We have calculated $(\Delta l/l)_{latt}$, with a Debye temperature $\theta_D=450$ K as used previously.[17,25] $[\Delta l/l(T)]_{latt}$ has been fitted to the experimental results in the paramagnetic regime; this leads to the overall temperature dependence of $[\Delta l/l(T)]_{latt}$ for each sample as shown by the dashed lines in Fig. 2(a). The anomalous magnetostriction $[\Delta l/l(T)]_m$ can be determined on subtraction of $[\Delta l/l(T)]_{latt}$ from the total experimental $\Delta l/l(T)$ (Ref. 25) with the resultant temperature dependences of $[\Delta l/l(T)]_m$ for $Dy_2Fe_{17-x}Mn_x$ with $x=0.0$, 1.0, and 3.0 shown as examples in Fig. 2(b). It can be seen that at low temperatures ($T<\sim 0.3\ T_C$), $[\Delta l/l(T)]_m$ decreases as the Mn content increases.

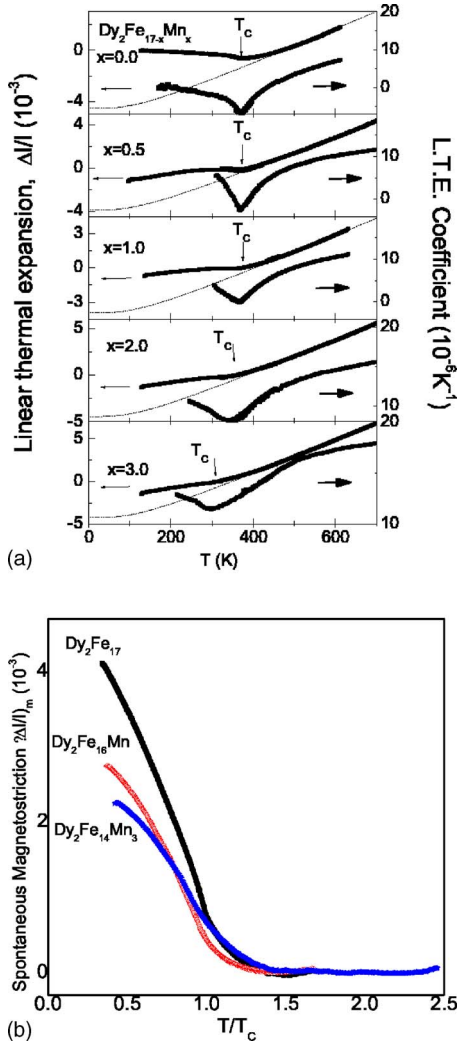

FIG. 2. (Color online) (a) Linear thermal expansion (LTE) and thermal dependence of the LTE coefficient of $Dy_2Fe_{17-x}Mn_x$ with $x=0$, 0.5, 1.0, 2.0, and 3.0. The dashed line represents the calculated nonmagnetic anharmonic phonon contribution as discussed in the text. (b) Temperature dependence of the spontaneous magnetostriction $[\Delta l/l(T)]_m$, for $Dy_2Fe_{17-x}Mn_x$ with $x=0$, 1.0, and 3.0.

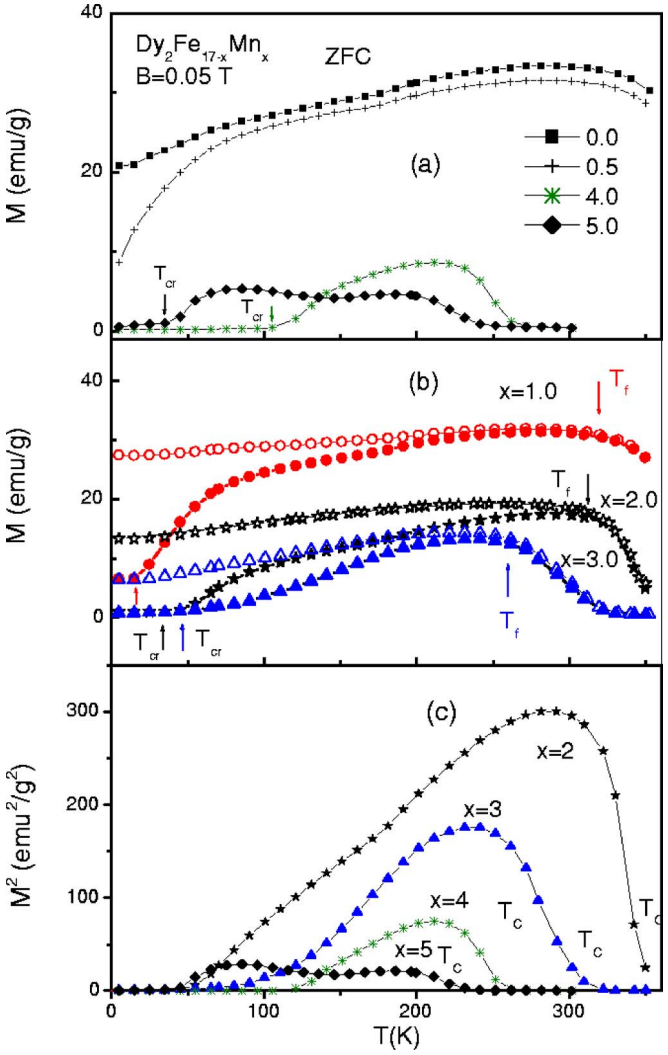

FIG. 3. (Color online) (a) Temperature dependence of magnetization measured in a field of $B_{appl}=0.05$ T for $Dy_2Fe_{17-x}Mn_x$ compounds with $x=0.0$, 0.5, 4.0, and 5.0 after zero-field cooling (ZFC). The critical temperatures T_{cr} are discussed in the text. (b) Temperature dependence of magnetization in a field of 0.05 T for $Dy_2Fe_{17-x}Mn_x$ with $x=1.0$, 2.0, and 3.0, in a ZFC (full symbols) and in a FC (empty symbols) process. The freezing temperatures T_f are discussed in the text. (c) Temperature dependence of the square of the magnetization for $Dy_2Fe_{17-x}Mn_x$ ($x=2.0$, 3.0, 4.0, and 5.0) as determined from the 0.05 T data of Figs. 3(a) and 3(b). The T_C values marked by arrows were obtained by extrapolation of the M^2 values to zero as described in the text.

It can also be seen that even in the paramagnetic phase, a considerable value of spontaneous magnetostriction is obtained, indicating the existence of strong short-range magnetic correlations above T_C.[17,25] The nonmonotonic behavior of the unit-cell volume for $x \leqslant 2$ noted above can therefore be understood by considering the magnetovolume effect in compounds for which the Curie temperature T_C is above or close to room temperature.

B. Magnetic properties

1. Magnetization (0–5 T)

Figures 3(a) and 3(b) show the temperature dependence of the magnetization for $Dy_2Fe_{17-x}Mn_x$ compounds as measured in an applied magnetic field of 0.05 T. The measurements were performed by increasing the temperature after samples were first cooled in zero magnetic field. As noted in Sec. II and as shown in Fig. 3(c), the Curie temperatures for those $Dy_2Fe_{17-x}Mn_x$ samples with T_C below 350 K ($x=2.0, 3.0, 4.0, 5.0$) were determined from M^2-T plots by extrapolating M^2 to zero. As shown in Table I, good agreement was obtained between the T_C values derived by the two methods—linear thermal expansion [Fig. 2(a)] and magnetization measurements [Fig. 3(c)]—for the two samples ($x=2.0, 3.0$) which overlap the temperature regions available for the different sets of apparatus.[25]

As is evident in Figs. 3(a) and 3(b), compounds with $x=2.0$, 3.0, 4.0, and 5.0 exhibit approximately constant magnetization values below a critical temperature T_{cr} after zero-

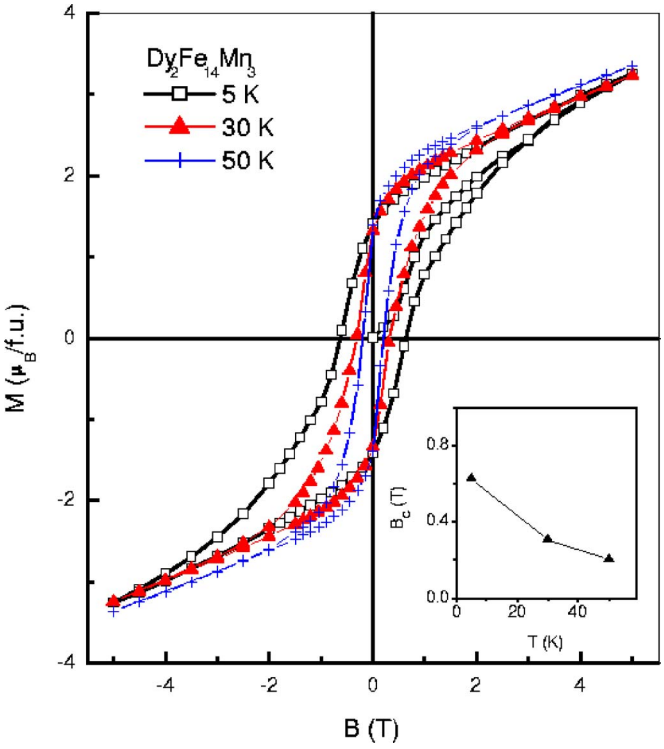

FIG. 4. (Color online) The initial magnetization curve at 5 K for a piece of $Dy_2Fe_{14}Mn_3$ ingot, and hysteresis loops at 5, 30, and 50 K. The inset shows the temperature dependence of the coercive field for $Dy_2Fe_{14}Mn_3$.

field cooling (ZFC). Figure 3(b) also shows comparisons of the temperature dependences of the magnetization of compounds with $x=1.0$, 2.0, and 3.0 after field cooling (FC) processes in a field of 0.05 T. A clear irreversibility appears at the freezing temperature T_f which can be ascribed to a pronounced magnetohistory effect.[17,26–28] The T_{cr} and T_f values are listed in Table I.

Magnetic hysteresis loop measurements provide a useful and effective tool for studying magnetic domain motion.[26,27] The initial magnetization curve for a small bulk sample of $Dy_2Fe_{14}Mn_3$ at 5 K along with hysteresis loops at 5, 30, and 50 K are shown in Fig. 4. A large magnetic hysteresis is observed at 5 K with a coercive field of $H_C=0.63$ T. This large magnetic hysteresis at low temperature is comparable to the cases of $Pr_2Fe_{17-x}Mn_x$,[28] $RCo_{5-x}Ni_x$ with R=Y and La,[29] $SmNi_4B$,[30] and RNi_2Mn.[27] With increasing temperature, the coercivity of the bulk sample decreases quickly (inset in Fig. 4) as a result of the increasing thermal energy.[28]

The spontaneous magnetization M_s at 5 K has been derived from Arrot plots of M^2 versus H/M for the free $Dy_2Fe_{17-x}Mn_x$ powder samples. As shown by the graph of M_s(5 K) versus Mn content in Fig. 5, the spontaneous magnetization M_s first decreases in an approximately linear manner to a minimum at about $x\sim4$ before increasing with further increase in the Mn content. The appearance of this minimum in the compositional dependence of M_s can be explained in terms of a compensation concentration originating from the ferrimagnetic coupling between the Dy and the 3*d*-sublattice magnetizations.[6,18,21] In R-T intermetallic compounds, it is well established that the indirect exchange interaction between the 3*d* spins of the T elements and the 4*f* spins of the R elements exhibits ferromagnetic coupling for light R elements (less than half-full 4*f* shell), and antiferromagnetic or ferrimagnetic coupling for heavy R elements (more than half-full 4*f* shell).[31–34] In agreement with these well established effects, $Dy_2Fe_{17-x}T_x$ and $Dy_2Co_{17-x}T_x$ compounds exhibit ferrimagnetism.[6,18,32,33] The transition-metal sublattice magnetization M_T can be obtained from the measured M_s by subtracting the rare-earth sublattice magnetization. We consider that the rare-earth sublattice magnetization is the same for all the compounds and has the same value as the free ion magnetic moment. The results of this calculation for M_T are shown in Fig. 5(a) with M_T found to exhibit a linear decrease with Mn content x (dashed line). For com-

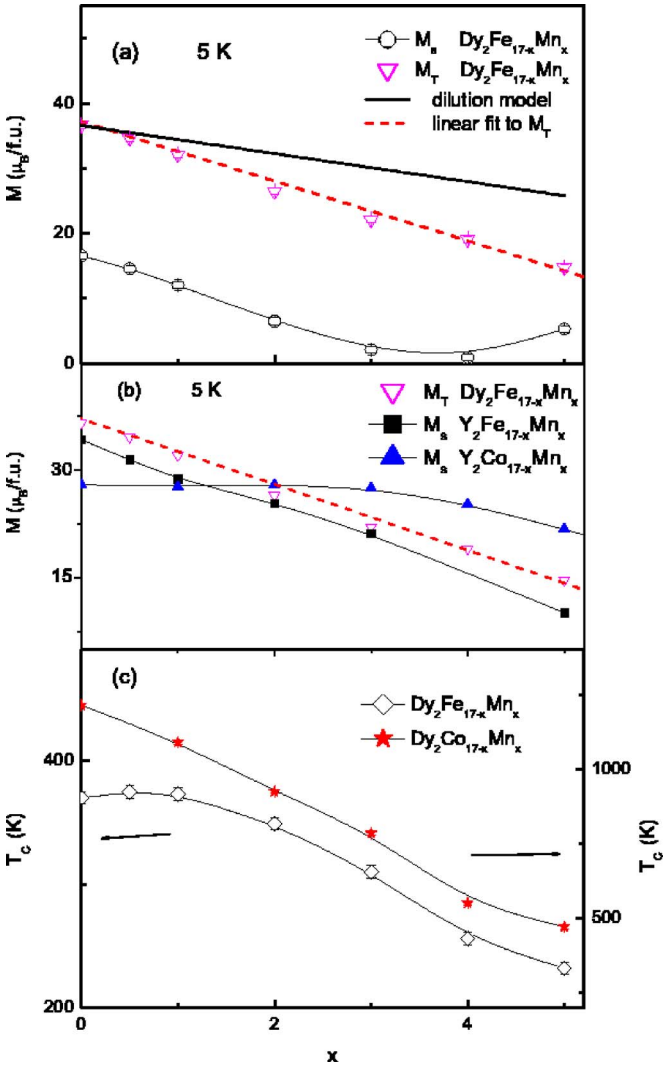

FIG. 5. (Color online) Composition dependence of the following. (a) The spontaneous magnetization M_s and the transition-metal sublattice moment M_T for $Dy_2Fe_{17-x}Mn_x$ at 5 K. The dashed line is a linear fit to M_T with the continuous line corresponding to the behavior expected from a dilution model (see text). (b) The M_T values for $Dy_2Fe_{17-x}Mn_x$ along with M_s for $Y_2Fe_{17-x}Mn_x$ (Ref. 35) and $Y_2Co_{17-x}Mn_x$ (Ref. 15). (c) The Curie temperatures T_C for $Dy_2Fe_{17-x}Mn_x$ (present work) and $Dy_2Co_{17-x}Mn_x$ (Ref. 18).

parison, the calculated composition dependence of M_T based on a simple dilution model represented by $[M_T(Dy_2Fe_{17-x}Mn_x)=M_T(Dy_2Fe_{17})(17-x)/17]$, in which the Mn atoms do not carry moment, is also shown in Fig. 5(a). It is clear that the observed decrease of M_T with increasing Mn content occurs more rapidly than that expected by this simple dilution model. Based on the fitting to the linear part in the composition dependence of M_s, it can be derived that for compounds with $x<4$ the substitution of Mn atoms for Fe leads to a decrease of M_s of around $4.6\mu_B$ per Mn atom. This suggests that the Mn atoms carry magnetic moments which should be antiparallel to the Fe moments. This assumption is supported by neutron-diffraction results obtained on the $Er_2Fe_{14-x}Mn_xB$ series where the presence of Mn induces antiferromagnetic coupling, not only between Mn moments and Fe moments but also between Fe moments.[31]

In order to aid comparison between the behaviors of $R_2Fe_{17-x}Mn_x$ and $R_2Co_{17-x}Mn_x$, the composition dependence of M_s for compounds $Y_2Fe_{17-x}Mn_x$ (Ref. 35) and $Y_2Co_{17-x}Mn_x$ (Ref. 15) (nonmagnetic R element) is first considered. Figure 5(b) shows that there is consistent agreement between M_T for $Dy_2Fe_{17-x}Mn_x$ and M_s for $Y_2Fe_{17-x}Mn_x$,[35] thus indicating the overall correctness of our calculation for M_T. The slightly reduced values of M_s for $Y_2Fe_{17-x}Mn_x$ compared with M_T for $Dy_2Fe_{17-x}Mn_x$ indicate that the value of M_{Dy} in $Dy_2Fe_{17-x}Mn_x$ may be smaller than $10\mu_B$, the free Dy ion magnetic moment.[6] By comparison, the M_s for $Y_2Co_{17-x}Mn_x$ [Fig. 5(b)] exhibits an approximately constant saturation magnetization for $x<3$, before decreasing with increasing Mn content.[15] It is accepted that the large spatial extent of the $3d$ wave functions leads to $3d$ electron energy bands rather than to a $3d$ level. Because the modification in the difference between the spin-up and spin-down states due to the substitution of Mn for Fe or Co reflects the saturation magnetization, the different changes of magnetization in $R_2Fe_{17-x}Mn_x$ and $R_2Co_{17-x}Mn_x$ compounds can be ascribed to the difference in the number of the outer electrons in Fe($3d^64s^2$), Mn($3d^54s^2$), and Co ($3d^74s^2$).

As shown in Fig. 5(c), the Curie temperatures for $Dy_2Fe_{17-x}Mn_x$ remain essentially unchanged for Mn contents up to $x=1$ before decreasing rapidly with further increase in Mn content. This behavior differs from that observed in $Dy_2Co_{17-x}Mn_x$ [see Ref. 18; also shown in Fig. 5(c) for comparison], $R_2Fe_{14-x}Mn_xC$,[36] and $R_2Fe_{14-x}Mn_xB$,[37] where Mn substitution for Fe or Co leads to a rapid decrease of T_C with the increase in the Mn content. In general, we can consider that T_C is determined by the strengths of the exchange interactions and by the $3d$-sublattice magnetization M_T. Among the three types of exchange interactions present in R-T intermetallics (T-T, R-T, and R-R), the T-T interactions are the strongest and the R-R interactions the weakest. The T-T interaction is sensitive to the distance between T-T atoms and represented by the exchange interaction constant, J_{TT}. According to the molecular-field approximation, if we consider only the T-T interaction, the relation between T_C, the T-T interaction, and the $3d$-sublattice magnetization M_T can be written as

$$3k_BT_C = J_{TT}Z_{TT}S_T(S_T+1). \quad (1)$$

Here, S_T is the so-called pseudospin, which is related to the $3d$-sublattice magnetization:[1]

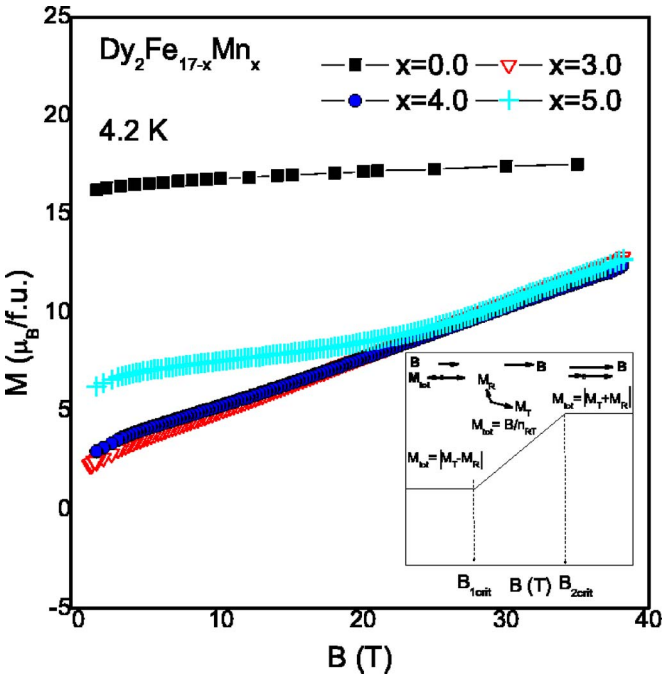

FIG. 6. (Color online) High-field magnetization curves of $Dy_2Fe_{17-x}Mn_x$ compounds at 4.2 K. The inset depicts the response of the transition-metal sublattice magnetization M_T and the rare-earth sublattice magnetization M_R configurations for ferrimagnetic R-T intermetallics of a two-sublattice system in various magnetic fields as discussed in the text. The B arrow represents the increase in magnetic field in the delineated regions ($0\ T<B<B_{1crit}$, $B_{1crit}<B_{2crit}$, $B_{2crit}<B<38$ T) with the orientations of M_T and M_R also depicted schematically.

$$M_T = -g_T\mu_B S_T. \quad (2)$$

In $Dy_2Fe_{17-x}Mn_x$ compounds with $x>2$, the decrease of T_C with further increase in Mn content can be considered as a result of the decrease of the $3d$-sublattice magnetization. In the case of $x\leqslant 2$, the essentially invariant nature of T_C [Fig. 5(b)] can be due to the competition between the variation of the strength of the T-T interaction and the variation of M_T with Mn content. This behavior can be related to the preferential occupation of the $6c/4f$ Fe sites by the Mn in this doping range which leads to an enhancement of the T-T interaction, as previously reported in the case of the $Nd_2Fe_{17-x}Mn_x$ compounds.[12]

2. *High-field magnetization* (0–38 T)

For collinear ferrimagnetic R-T intermetallics, Verhoef[19] studied the high-field magnetization behavior of free powder (HFFP) samples of the heavy R-T compounds. Assuming that the $3d$ sublattice anisotropy is zero, and also that the sample is free to rotate in the sample holder, it was found that for applied magnetic field values in the interval $B_{1crit}<B<B_{2crit}$ (where $B_{1crit}=n_{RT}|M_R-M_T|$, $B_{2crit}=n_{RT}|M_R+M_T|$, and n_{RT} is the intersublattice molecular coefficient), a canted-moment configuration exists and the magnetization depends linearly on the field with a slope of $1/n_{RT}$ ($M=B/n_{RT}$; see inset in Fig. 6). When both sublattice moments M_R and M_T are equal, the straight line describing the

magnetic-field dependence of the magnetization passes through the origin of the magnetization isotherm. So, by means of HFFP magnetization measurements, the values of n_{RT} can be derived in a relatively straightforward manner. Since the Fe-sublattice moment is larger than the R-sublattice moment in Dy_2Fe_{17}, the substitution of Mn for Fe leads to a decrease of the difference between the moments of the Dy and T sublattices and at a certain composition, B_{1crit} can be reached. Figure 6 shows that for $Dy_2Fe_{12}Mn_5$ the magnetization is approximately constant for $B<B_{1crit}$ $\sim$25 T, but for $B>B_{1crit}$ the magnetization increases nearly linearly with increasing applied field. From the slope of the linear regions of the magnetization curves shown in Fig. 6, the values of n_{RT} were determined to be 3.61, 3.91, and 3.96 T f.u./μ_B for $Dy_2Fe_{17-x}Mn_x$ samples with Mn contents $x=3$, 4, and 5 respectively (Table I).

If we consider only nearest-neighbor exchange interactions and assume that the R-T exchange coupling is spatially isotropic,[6,19] the microscopic R-T exchange-coupling constant, J_{RT}, is related to the macroscopic intersublattice molecular-field coefficient n_{RT} via the following expression:

$$J_{RT} = -\frac{N_T g_R \mu_B^2}{Z_{RT}(1-g_R)} n_{RT}, \tag{3}$$

where $N_T=17$ is the number of T (Fe and Mn) atoms per formula unit and $Z_{RT}=19$ is the number of T neighbors of an R atom.[6] The values of J_{RT} in $Dy_2Fe_{17-x}Mn_x$ were derived to be −8.68, −9.41 and −9.48 K for $x=3$, 4, and 5 respectively. Similar to the cases of $Dy_2Fe_{17-x}Al_x$ and $Dy_2Fe_{17-x}Ga_x$,[38,39] these $Dy_2Fe_{17-x}Mn_x$ compounds all exhibit absolute values for J_{RT} larger than that in Dy_2Fe_{17} (−7.0 K).[6,32]

C. Mössbauer spectroscopy

Figures 7 and 8 show the ^{57}Fe Mössbauer spectra of $Dy_2Fe_{16}Mn_1$ and $Dy_2Fe_{14}Mn_3$, respectively, at selected temperatures. The spectra have been fitted with a self-consistent model[40] taking into account the orientation of the iron magnetic moments, the correlation between the iron isomer shifts and the Wigner-Seitz cell volumes, and the correlation between the hyperfine fields and the number of iron near neighbors. As there are four different crystallographic sites for Fe in both the hexagonal- and rhombohedral-type R_2Fe_{17} compounds,[40] the observed spectrum must be a superposition of at least four sextets. Point-charge calculations showed that under the combined effects of the dipolar field and the quadrupole interaction, only the dumbbell $4f$ ($6c$) sites remain equivalent since the angle between the hyperfine field and the electric-field-gradient tensor is zero. The hyperfine parameters are different at various crystallographically inequivalent sites.[41] This leads to a total of seven subspectra: $4f$ ($6c$), $6g1$ ($9d1$), $6g2$ ($9d2$), $12j1$ ($18f1$), $12j2$ ($18f2$), $12k1$ ($18h1$), and $12k2$ ($18h2$) with intensity ratios 4 (6):4 (6):2 (3):8 (12):4 (6):8 (12):4 (6) corresponding to the site occupancies of Fe atoms in the crystal structure of R_2Fe_{17} with planar anisotropy. In the present study, due to the large number of sextets, some constraints were adopted during the process of fitting. The intensities of the six absorption lines of each sextets were assumed to follow the 3:2:1 intensity ratio expected for randomly oriented powder samples in zero magnetic field and a single common linewidth was assumed for all the seven sextets. The isomer shifts for the magnetically inequivalent sites were constrained to be the same, whereas the hyperfine fields are expected to be slightly different at pairs of magnetically inequivalent sites as a result of variations in the dipolar and orbital contributions to the magnetic hyperfine fields. Because the Mn atoms preferentially occupy a particular iron site[11,12,16] and this does not depend

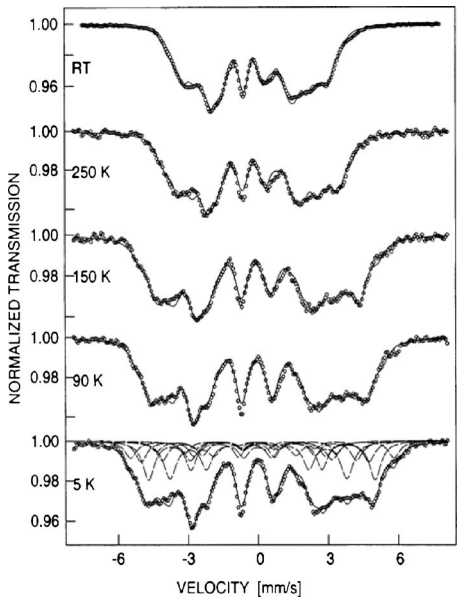

FIG. 7. ^{57}Fe Mössbauer spectra of $Dy_2Fe_{16}Mn_1$ over the temperature range 5–300 K. The fits to the spectra (continuous lines) are described in the text.

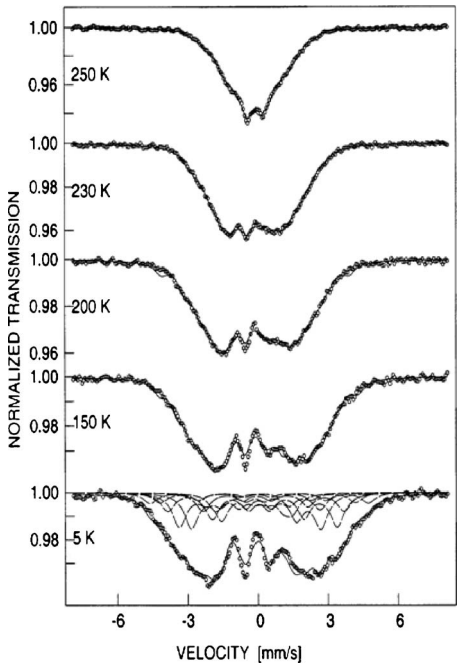

FIG. 8. ^{57}Fe Mössbauer spectra of $Dy_2Fe_{14}Mn_3$ over the temperature range 5–300 K. The fits to the spectra (continuous lines) are described in the text.

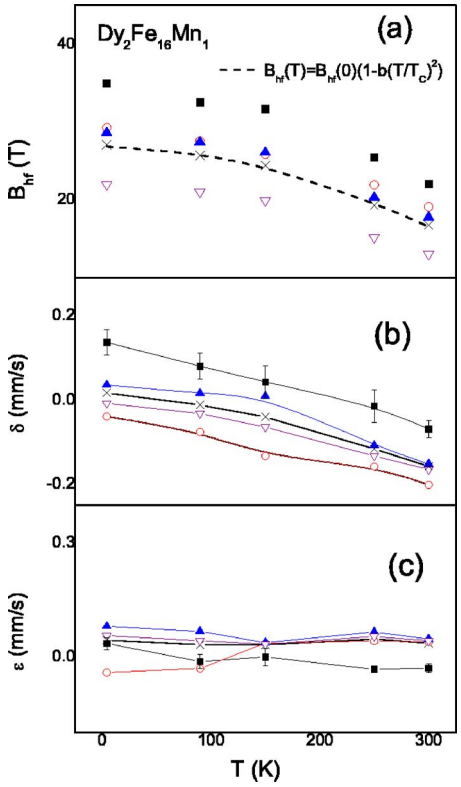

FIG. 9. (Color online) Temperature dependences of the average Mössbauer hyperfine parameters of $Dy_2Fe_{16}Mn_1$ (cross symbol x) along with the individual site values (symbols: solid square ■, open circle ○, solid up-triangle ▲, and open down-triangle ▽ represent the behavior of the 4*f*, 6*g*, 12*j*, and 12*k* sites, respectively). (a) Magnetic hyperfine field B_{hf} (the dashed line represents a fit to the average values (cross symbol x) as discussed in the text). (b) Quadrupole shift ε. (c) Isomer shift δ. The continuous lines are guides for the eyes.

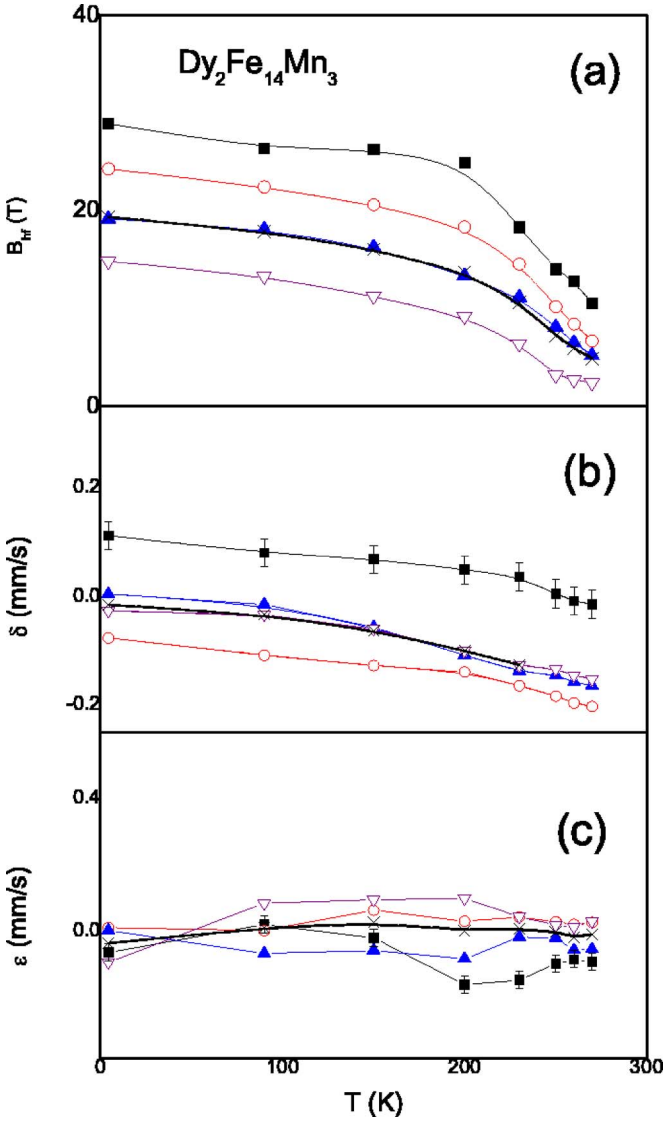

FIG. 10. (Color online) Temperature dependences of the average Mössbauer hyperfine parameters of $Dy_2Fe_{14}Mn_3$ (cross symbol ×) along with the individual site values (symbols: solid square ■, open circle ○, solid up-triangle ▲, and open down-triangle ▽ represent the behavior of the 4*f* (6*c*), 6*g* (9*d*), 12*j* (18*f*), and 12*k* (18)*h* sites, respectively). (a) Magnetic hyperfine field B_{hf}. (b) Quadrupole shift ε. (c) Isomer shift δ. The continuous lines are guides for the eyes.

on the R element, the corresponding Fe content at inequivalent sites for $Dy_2Fe_{17-x}Mn_x$ has been calculated by using the Mn occupancy factor for $Nd_2Fe_{17-x}Mn_x$ and $Ce_2Fe_{17-x}Mn_x$ compounds obtained from neutron-diffraction studies.[12,16] The corresponding intensity ratios for the Mössbauer subspectra have been modified for $Dy_2Fe_{16}Mn_1$ and $Dy_2Fe_{14}Mn_3$. Emphasis was placed on fitting the 5 K spectrum and the final parameters used as the basis for the initial parameters in the analysis of the higher-temperature spectra. Examples of the resultant fits (continuous lines) are shown in Figs. 7 and 8 for $Dy_2Fe_{16}Mn_1$ and $Dy_2Fe_{14}Mn_3$, respectively. As examples, the individual subspectra which comprise the final fits are shown for the 5 K spectra in Figs. 7 and 8.

Figures 9 and 10 show the temperature dependences of the Mössbauer hyperfine parameters of $Dy_2Fe_{16}Mn$ and $Dy_2Fe_{14}Mn_3$, respectively. The assignments of the subspectra were performed by taking into account the nearest-neighbor environment of each respective site and the Fe-Fe distances.[40,41] The hyperfine field sequences 4*f* (6*c*) > 6*g* (9*d*) > 12*j* (18*f*) > 12*k* (18*h*) have been observed to be similar to the sequence observed in other R_2Fe_{17} compounds.[40,41] As shown in Fig. 9, the temperature dependence of the average hyperfine field for $Dy_2Fe_{16}Mn_1$ can be well fitted by the equation[42,43]

$$B_{hf}(T) = B_{hf}(0)\left[1 - b\left(\frac{T}{T_C}\right)^2\right]. \quad (4)$$

The value of the hyperfine field at 5 K has been taken as $B_{hf}(0)$ and the fitted value of the constant b is 0.58. The temperature dependence of the hyperfine fields for $ErFe_{12-x}Nb_x$ or other R_2Fe_{17}-based compounds also follows the above equation with $b=0.5$ for R_2Fe_{17} (R=Y, Nd, and Dy),[42,43] $b=0.53$ for $HoErFe_{15}Ga_2$,[40] and $b=0.46$ for $ErFe_{11.4}Nb_{0.6}$.[44] The T^2 dependence of the hyperfine fields in the present series of compounds suggests that single-particle excitations may be responsible for suppressing the 3*d*-sublattice magnetization with increasing temperature.[40,43]

The correlation between the ^{57}Fe isomer shift δ and the WSC volume available to the iron atoms in R_2Fe_{17} and $RFe_{11}Ti$ and their interstitial compounds has proved to be very successful in delineating the electronic structure of these compounds.[40,41,44] Given the lack of detailed information on the structural and positional parameters for $Dy_2Fe_{17-x}Mn_x$, we have calculated the WSC volumes with the BLOKJE program[45] for all the crystallographic sites in $Ce_2Fe_{16}Mn$ and $Ce_2Fe_{14}Mn_3$ by using the structural and positional parameters[16] and the 12-coordinated metallic radii of 1.81, 1.26, and 1.35 Å for Ce, Fe, and Mn, respectively. The calculated WSC volumes for the 6*c*, 9*d*, 18*f*, and 18*h* sites in $Ce_2Fe_{16}Mn$ ($Ce_2Fe_{14}Mn_3$) are 12.11 (12.15), 11.55 (11.54), 11.45 (11.49), and 11.00 (11.11) Å^3, respectively. Using these WSC volumes as a guide for the present $Dy_2Fe_{17-x}Mn_x$ compounds, it can be seen from Figs. 9 and 10 that the relations $\delta_{6c(4f)} > \delta_{18f(12j)} \approx \delta_{18h(12k)} > \delta_{9d(6g)}$ are obeyed at all temperatures; this agrees with the relationship between the isomer shift and the WSC volumes (the larger the WSC volume, the larger the isomer shift δ). Moreover, the 6*c* (4*f*), 18*f* (12*j*), 18*h* (12*k*), and 9*d* (6 *g*) sites and the site-averaged isomer shift increase with decreasing temperature.

IV. CONCLUSIONS

A positive spontaneous magnetostriction has been found below the ordering temperature for $Dy_2Fe_{17-x}Mn_x$ compounds for $x=0-5$ (Fig. 2). This strong magnetovolume effect leads to a slight maximum around $x=0.5$ of the composition dependence of the unit-cell volume at room temperature (Fig. 1). The invarlike effect evident around room temperature in $Dy_2Fe_{17-x}Mn_x$ compounds can account for the nonmonotonic composition dependence of the lattice parameters at room temperature compared with other $R_2Co_{17-x}Mn_x$ and $R_2Fe_{17-x}M_x$ systems (M=Al, Ga, and Si). The 3*d*-sublattice magnetization in $Dy_2Fe_{17-x}Mn_x$ decreases monotonically with increasing the Mn content (Fig. 5). The Curie temperature remains essentially unchanged at low Mn doping rates but rapidly decreases with further increase of the Mn content. This variation can be explained in terms of the composition dependence of the 3*d*-sublattice magnetization and the strength of the T-T interaction. The compounds with $x \leqslant 1.0$ show pronounced magnetic history effects which are ascribed to the presence of narrow domain walls.[46] The observed T^2 dependence of the ^{57}Fe hyperfine field for $Dy_2Fe_{16}Mn_1$ indicates that the reduction of the Fe-sublattice magnetization observed when the temperature increases is associated with a single-particle excitation mechanism. The average hyperfine fields at 5 K decrease with increasing Mn content with the hyperfine fields in the individual sites behaving as $4f\ (6c) > 6g\ (9d) > 12j\ (18f) > 12k\ (18h)$.

ACKNOWLEDGMENTS

We thank J. C. P. Klaasse for his help with the high-field measurements. This work is supported in part by a Discovery Grant from the Australian Research Council.

[1] H. S. Li and J. M. D. Coey, in *Handbook of Magnetic Materials*, edited by K. H. J. Buschow (North-Holland, Amsterdam, 1991), Vol. 6, p. 1.
[2] D. Zhang, C. H. de Groot, E. Bruck, F. R. de Boer, and K. W. J. Buschow, J. Alloys Compd. **259**, 42 (1997).
[3] Z. H. Cheng, B. G. Shen, Q. W. Yan, H. Q. Guo, D. F. Chen, C. Gou, K. Sun, F. R. de Boer, and K. H. J. Buschow, Phys. Rev. B **57**, 14299 (1998).
[4] Y. M. Hao, Y. Gao, B. W. Wang, J. P. Qu, Y. X. Li, J. F. Hu, and J. C. Deng, Appl. Phys. Lett. **78**, 3277 (2001).
[5] B. G. Shen, Z. H. Cheng, B. Liang, H. Q. Guo, J. X. Zhang, H. Y. Gong, F. W. Wang, Q. W. Yan, and W. S. Zhan, Appl. Phys. Lett. **67**, 1621 (1995).
[6] F. M. Yang, J. L. Wang, Y. H. Gao, N. Tang, X. F. Han, H. G. Pan, Q. A. Li, J. F. Hu, J. P. Liu, and F. R. de Boer, J. Appl. Phys. **79**, 7883 (1996).
[7] F. W. Wang, B. G. Shen, P. L. Zhang, Z. H. Cheng, J. X. Zhang, H. Y. Gong, B. Liang, X. D. Sun, and Q. W. Yan, J. Appl. Phys. **83**, 3250 (1998).
[8] J. L. Wang, R. W. Zhao, N. Tang, W. Z. Li, Y. H. Gao, F. M. Yang, and F. R. de Boer, J. Appl. Phys. **76**, 6740 (1994).
[9] B. G. Shen, H. Y. Gong, B. Liang, Z. H. Cheng, and J. X. Zhang, J. Alloys Compd. **229**, 257 (1995).
[10] J. L. Wang, F. R. de Boer, X. F. Han, N. Tang, C. Zhang, D. Zhang, E. Bruck, and F. M. Yang, J. Alloys Compd. **284**, 289 (1999).
[11] W. B. Yelon, Z. Hu, M. Chen, H. Luo, P. C. Ezekwenna, G. K. Marasinghe, W. J. James, K. H. J. Buschow, D. P. Middleton, and F. Pourarian, IEEE Trans. Magn. **32**, 4431 (1996).
[12] P. C. Ezekwenna, G. K. Marasinghe, W. J. James, O. A. Pringle, Gary J. Long, H. Luo, Z. Hu, W. B. Yelon, and Ph. l'Heritier, J. Appl. Phys. **81**, 4533 (1997).
[13] Y. G. Wang, F. M. Yang, C. P. Chen, N. Tang, P. H. Lin, and Q. D. Wang, J. Appl. Phys. **84**, 6229 (1998).
[14] Z. G. Sun, H. W. Zhang, J. Y. Wang, and B. G. Shen, J. Appl. Phys. **86**, 5152 (1999).
[15] Z. G. Sun, H. W. Zhang, B. Liang, J. Y. Wang, B. G. Shen, and J. P. Liu, J. Appl. Phys. **87**, 5311 (2000).
[16] A. G. Kuchin, A. N. Pirogov, V. I. Khrabrov, A. E. Teplykh, A. S. Ermolenko, and E. V. Belozerov, J. Alloys Compd. **313**, 7 (2000).
[17] J. L. Wang, M. R. Ibarra, C. Marquina, and B. García-Landa, W. X. Li, N. Tang, W. Q. Wang, F. M. Yang, and G. H. Wu, J. Appl. Phys. **92**, 1453 (2002).
[18] Y. B. Li, L. G. Zhang, S. Y. Zhang, and B. G. Shen, Chin. Phys. **11**, 174 (2002).
[19] R. Verhoef, Ph.D. thesis, University of Amsterdam, 1990.
[20] Z. G. Zhao, X. Li, J. H. V. J. Brabers, P. F. de Châtel, F. R. de Boer, and K. H. J. Buschow, J. Magn. Magn. Mater. **123**, 74 (1993).
[21] F. R. de Boer and Z. G. Zhao, Physica B **211**, 81 (1995).

[22] J. Rodriguez-Carvajal, Abstracts of the Satellite Meeting on Powder Diffraction of the XV Congress of the IUCr, Toulouse, France, 1990 (unpublished), p. 127 (http://www-llb.cea.fr/fullweb/)
[23] J. Shen, P. Qian, and N. X. Chen, Modell. Simul. Mater. Sci. Eng. **13**, 239 (2005).
[24] P. Qian, N. X. Chen, and Jiang Shen, Phys. Lett. A **335**, 464 (2005).
[25] L. Morellón, L. Pareti, P. A. Algarabel, B. García-Landa, M. R. Ibarra, F. Albertini, A. Paoluzi, and L. Pareti, Proceedings of the Eighth International Symposium on Magnetic Anisotropy and Coercivity in Rare-Earth Transition Metal Alloys Birmingham, 1994 (unpublished), p. 361.
[26] Z. R. Yang, S. Tan, and Y. H. Zhang, Appl. Phys. Lett. **79**, 3645 (2001).
[27] J. L. Wang, C. C. Tang, G. H. Wu, Q. L. Liu, N. Tang, W. Q. Wang, W. H. Wang, F. M. Yang, J. K. Liang, F. R. de Boer, and K. H. J. Buschow, Solid State Commun. **121**, 615 (2002); J. L. Wang, C. Marquina, M. R. Ibarra, and G. H. Wu, Phys. Rev. B **73**, 094436 (2006).
[28] Z. G. Sun, S. Y. Zhang, H. W. Zhang, and B. G. Shen, J. Alloys Compd. **349**, 1 (2003).
[29] H. Oesterricher, F. T. Parker, and M. Misroch, Solid State Commun. **19**, 539 (1976).
[30] Chandan Mazumdar, R. Nagarajan, L. C. Gupta, B. D. Padalia, and R. Vijayaraghavan, Appl. Phys. Lett. **77**, 895 (2000).
[31] C. D. Fuerst, F. P. Meisner, F. E. Pinkerton, and W. B. Yelon, J. Appl. Phys. **63**, 3119 (1988).
[32] J. P. Liu, F. R. de Boer, P. F. de Châtel, R. Coehoorn, and K. H. J. Buschow, J. Magn. Magn. Mater. **132**, 159 (1994).
[33] N. Tang, J. L. Wang, Y. H. Gao, W. Z. Li, F. M. Yang, and F. R. De Boer, J. Magn. Magn. Mater. **140**, 979 (1995).
[34] D. Cakmak, A. Elmali, Y. Elerman, and O. Cakir, Solid State Commun. **131**, 241 (2004).
[35] N. M. Hong, N. P. Thuy, and J. J. M. Franse, Physica B **153**, 53 (1988).
[36] R. Verhoef, F. R. de Boer, J. J. M. Franse, C. J. M. Denissen, T. H. Jacobs, and K. H. J. Buschow, J. Magn. Magn. Mater. **80**, 41 (1989).
[37] C. D. Fuerst, G. P. Meisner, and F. E. Pinkerton, J. Appl. Phys. **61**, 2314 (1987).
[38] T. H. Jacobs, K. H. J. Buschow, F. Zhou, and F. R. de Boer, Physica B **179**, 177 (1992).
[39] N. Sheloudko, A. Gilewski, X. L. Rao, V. Skumryev, and J. S. Muñoz, J. Magn. Magn. Mater. **231**, 157 (2001).
[40] M. Venkatesan, U. V. Varadaraju, and K. V. S. Rama Rao, Phys. Rev. B **64**, 094427 (2001).
[41] F. Grandjean, O. Isnard, and G. J. Long, Phys. Rev. B **65**, 064429 (2002).
[42] J. J. M. Franse and R. J. Radwanski, in *Handbook of Magnetic Materials*, edited by K. H. J. Buschow (North-Holland, Amsterdam, 1993), Vol. 7, p. 307.
[43] P. C. M. Gubbens and K. H. J. Buschow, J. Phys. F: Met. Phys. **12**, 2715 (1982).
[44] J. L. Wang, S. J. Campbell, J. M. Cadogan, O. Tegus, and A. V. J. Edge, J. Phys.: Condens. Matter **17**, 3689 (2005).
[45] L. Gelato, J. Appl. Crystallogr. **14**, 151 (1981).
[46] T. H. Jacobs, K. H. J. Buschow, R. Verhoef, and F. R. de Boer, J. Less-Common Met. **157**, L11 (1990).